International Journal of GEOMATE, Sept. 2022, Vol.23, Issue 97, pp.220-227
ISSN: 2186-2982 (P), 2186-2990 (O), Japan, DOI: https://doi.org/10.21660/2022.97.j2375
Geotechnique, Construction Materials, and Environment

CHARACTERIZATION OF THE MAMASA EARTHQUAKE SOURCE BASED ON HYPOCENTER RELOCATION AND GRAVITY DERIVATIVE DATA ANALYSIS

*Mohammad Syamsu Rosid[1], Yusuf Haidar Ali[1,2], and Mohamad Ramdhan[3]

[1]Physics Department, FMIPA Universitas Indonesia, Indonesia; [2]Indonesian Agency for Meteorology, Climatology, and Geophysics, Indonesia; [3]Research Center for Geological Disaster, National Research and Innovation Agency (BRIN), Bandung, 40135, Indonesia

*Corresponding Author, Received: 22 Oct. 2021, Revised: 12 June 2022, Accepted: 03 July 2022

ABSTRACT: Mamasa, located in West Sulawesi, Indonesia, is a populous dense area with a low seismic hazard. In this area, the question of fault reactivation was raised due to the 804 reported earthquakes from November 2018 to February 2019. This series does not show an apparently major earthquake or behaviors, such as swarms. One month earlier, on 28 September 2018, the 7.6 Mw Palu earthquake occurred at a distance of approximately 230 km north of Mamasa. It affected the occurrence of this swarm since Mamasa has many hydrothermal manifestations, which have been linked with seismic activity. To investigate the roles of these two factors, the series of earthquakes and their possible linked faults must be characterized. Specifically, the double-difference hypocenter relocation method was used to relocate the earthquakes and conduct a spatiotemporal analysis of this swarm. Furthermore, the FHD (first horizontal derivative) gravity data were used to illuminate the possible linked fault. To assess the impact of the Palu earthquake, the Coulomb stress was calculated, and it was reported that it was very small. Therefore, it played an insignificant role in triggering the swarm. In contrast, the relocated earthquakes are concentrated in an area surrounded by surface hydrothermal manifestations, and the swarm feature is consistent with the interpretation of associated seismicity. Therefore, hydrothermal activities play a critical role in triggering the swarm.

Keywords: Earthquake Characterization, Earthquake Relocation, FHD Gravity, Coulomb Stress

1. INTRODUCTION

High seismicity occurring in areas with low seismicity records is a phenomenon that needs to be investigated. Earthquake swarms are series that are formed without a specific mainshock. They are caused by volcanic activity [1,2] and fluid movement in the hydrothermal system [3] and geothermal system [4]. Furthermore, earthquake swarm activity can occur in active fault areas [5]. Based on the BMKG (Indonesian Agency for Meteorology, Climatology, and Geophysics) repository, there is an average of only one earthquake per month in the Mamasa region. Therefore, this region can be classified as a low-seismicity area. However, from November 2018 to February 2019, the BMKG recorded an 804 earthquake sequence, which had no discernible mainshock in the eastern part of the regency. This sequence had characteristics that resulted in its name, the Mamasa earthquake swarm.

A previous study on this series concluded that the earthquakes were caused by local faults due to a dominant downward mechanism [6]. However, there are many hydrothermal manifestations in the Mamasa region that may also have a significant role in this earthquake sequence. In contrast, the Palu great earthquake sequence occurred approximately one month before the Mamasa earthquake swarm. The triggering between these earthquakes needs to be investigated to comprehensively identify the causes of the swarm sequence. Therefore, this study aims to identify the causes of the Mamasa earthquake swarm, which are important for seismic hazard assessment. This evaluation was conducted using 83,899 residents from 6 and 2 districts in the Mamasa and Tana Toraja Regencies [7] in this seismic zone.

Three analyses were conducted to conclude the triggers of this earthquake sequence. First, earthquake relocation was conducted using the double-difference method [8], and a local velocity model was obtained by Velest [9]. Second, the analysis of the first horizontal derivative (FHD) of high-resolution satellite gravity data was used to obtain fault alignment [10]. Finally, the static pressure was analyzed to find the presence of external factors that may trigger a series of earthquakes in the Mamasa region.

2. RESEARCH SIGNIFICANCE

This study is important to understand the current background of seismicity in the Mamasa area. The role of hydrothermal activity and Palu earthquake activity in triggering earthquake swarms was investigated by using three different data analyses. In addition, we also conducted an initial seismic hazard assessment based on existing geological data. Therefore, the results of this study may be useful for local governments as initial data in earthquake disaster mitigation.

3. DATA AND METHODS

The data of the 1-D velocity model were derived by Velest [9], with Crust1.0 for the initial velocity [11]. Crust1.0 was chosen as an input because it is a global velocity model with a one-degree grid. Furthermore, it contains 5 layers of average depth and velocity of the two grids at 119.5 E 2.5 S and 119.5 E 3.5 S. The initial hypocenters of the Mamasa earthquake swarm were located in these two grids. In addition, more layers were added from iasp91 [12] for velocities below 35 km to constrain the mantle and the layer below it. The other Velest input consists of earthquake arrival time data from the BMKG catalog from November 2018 to February 2019 at coordinates 118.7 E – 120.3 E and 3.76 S – 2.45 S. These data were obtained based on azimuthal gap criteria of less than 180 degrees to obtain good initial hypocenter data. A total of 3316 P-phases and 1308 S-phases were used for this computation, and the initial and updated velocity model can be observed in Table 1 and Figure 1b.

Table 1. The initial and updated 1-D velocity models. The *V*p/*V*s value is 1.73.

No	Layer	Depth (km)	Initial *V*p (km/s)	Updated *V*p (km/s)
1	Sediment	Above 0.7–0.7	2.30	2.30
2	Upper Crust	0.7–11.3	5.80	6.01
3	Middle Crust	11.3–21.6	6.30	6.50
4	Lower Crust	21.6–31.9	6.90	6.77
5	Mantle Top	31.9–35	7.92	7.85
6	Constrained Layer	35–Below 35	8.08	7.93

The selection of 383 from 804 earthquakes that had an azimuth gap less than 180 degrees for hypocenter relocation (Figure 1a) with the updated velocity model was conducted, as shown in Table 1. The relocated hypocenter can be found in the supplementary data, and there were 373964 P-phase and 141976 S-phase pairs used for input to hypoDD. Furthermore, 365 earthquakes were relocated with residuals to a recording station between -0.67 milliseconds and 0.66 milliseconds and a final CND (condition number of double-difference) value of 41. A comparison of residual graphs before and after the earthquake is shown in Figure 1c and Figure 1d.

Gravity processing and topographic data were obtained from the GGM plus (Global Gravity Model) [13] and the SRTM (Shuttle Radar Topography Mission) [14]. They were then corrected by latitude correction using the 1967 EGRM formula, free air correction, Bouguer correction with the Parasnis method density [15], and terrain correction with a 200 m inner core and 1000 m outer core. In addition, the FHD was used to obtain different fault lines.

The focal mechanism parameter data from the selected foreshock, mainshock, and aftershock Global Centroid Moment Tensor (CMT) catalog were used as input for static stress modeling [16]. Additionally, Coulomb 3.3 was used for modeling the static stress [17]. The fracture plane modeling for each earthquake uses the empirical formula of magnitude correlation and plane fault [18]. It produces a map of the compression region represented by the red and the tension area of the blue region.

4. RESULTS AND DISCUSSION

The seismicity after the relocation formed a north–south trend with the direction reversing from N8W to northwest–southeast (Figure 2). Moreover, the azimuth value of 171.82 degrees is interpreted as the dominant strike of the local fault in the area, and the AB cross-section is constructed perpendicular to the dominant strike based on seismicity (Figure 2b). Therefore, the earthquake, which originally had a fixed depth of 10 km (Figure 2c), spread and tended to form a dip (Figure 2d) with an angle of approximately 53° to the east. The estimated local fault is verified by the results of Supendi et al. [6] and is directed eastward at an angle of 45°. The strike of this local fault is not aligned with the geological Sadang Fault. The predicted local and Sadang Faults are parallel to each other. Mamasa's seismicity is spread west of the Sadang Fault. It may be correlated with the Sadang Fault or as two different faults.

Hypocenter distributions are limited in forming dip angle patterns and spreading horizontally. The distribution of the hypocenter of the earthquake causes the zone to exhibit the complexity of the swarm. This differs from previous studies that showed a clear dip angle of a single local fault [6]. In contrast, earthquake swarms usually have a reduced zone due to hydrothermal activity [3]. Therefore, the colors for plotting earthquakes below M 3, which are classified as having small magnitudes, were clearly differentiated (Figure 2a-d). The location of hot spring manifestations [19] is near the seismicity area of the relocated earthquake for both small- and large-magnitude earthquakes (Figure 2b). Therefore, the distribution of the earth-

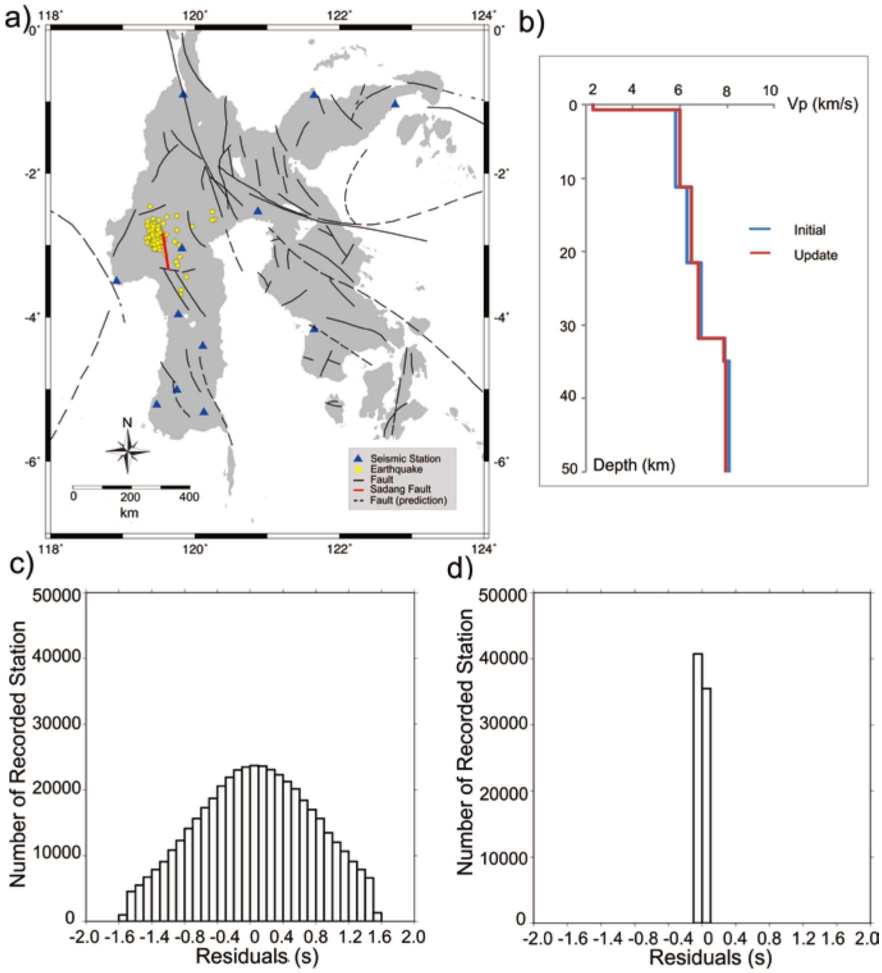

Fig. 1a) Seismicity map with earthquakes and seismic stations for Velest and HypoDD. b) Profile of the initial and updated local velocity model. c) Initial residual. d) Residual of relocated earthquakes with updated HypoDD velocity models.

quake hypocenter was strongly influenced by hydrothermal activity in this area. In addition, this earthquake swarm migrates to the northwest and southwest at the beginning of this series and randomly spreads thereafter (Figure 2e). This does not clearly show fluid migration since it was reported that fault activity is more prevalent than hydrothermal activity in this Mamasa earthquake swarm system.

The distribution of the earthquake hypocenter was strongly influenced by a combination of strike-slip and normal fault movements. The strike-slip fault movement is more dominant (Figure 2f). The dominance of this shear fault is shown by the results of the temporal spatial analysis at the beginning of the sequence. The normal fault in the earthquake swarm system usually shows an opening due to fluid migration in the area [1]. Mamasa's opening, which represents the explosive moment tensor, is associated with divergence movement. Explosive components may indicate the presence of hydrothermal activity. This is because hot water/steam has a mobile and divergent movement. Therefore, there is a large possibility that divergence movement occurred and triggered the events through the structures. This reinforces the previous assumption that hydrothermal activity also significantly adds to fault activity.

4.1 Gravity Result

On the CBA map, the low-anomaly zone, which is marked in blue (Figure 3a), shows the existence of a basin in the Mamasa region. It is the Sadang River valley area, and the CBA results can be found in the supplementary data. A river valley is characterized by at least two parameters, namely, the low lying areas of land between hills or mountains and alluvial sediments deposited along the watershed [20]. These two parameters cause the gravity anomaly to be low.

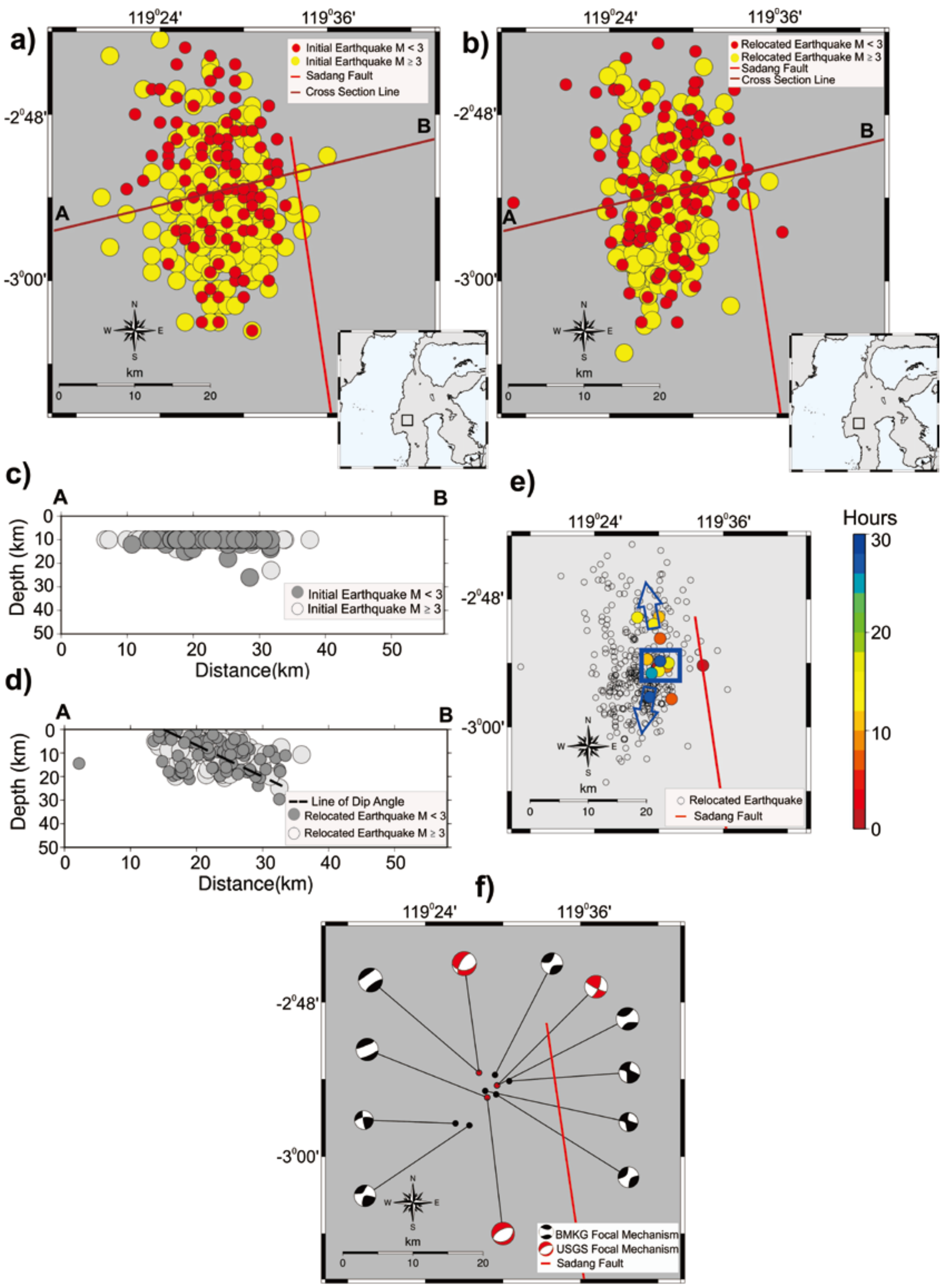

Fig. 2a) Seismicity map of initial earthquake locations. b) Seismicity map of relocated earthquakes. c) Cross-section of the initial earthquake. d) Cross-section of relocated earthquakes. e) Map of intertime seismicity. f) Focal mechanism map based on the location of the hypocenter.

The FHD results in this zone forming an area with maximum values, which are interpreted as lineaments of the Sadang Fault. The fault line shown in Figure 3b is similar to the results of Hamilton [21]. The fault line is in the fault location and strikes northwest–southeast. The result of the dominant gravity alignment of Suhanto and Bakrun [22] is almost in the north–south direction. Therefore, the FHD result successfully confirmed the existence and location of the Sadang Fault, which is strongly associated with the existing basin structure. Morphologically, the seismicity zone is situated on the Sadang River valley, as verified by the low gravity anomaly. The river may represent the existence of a structure [23,24].

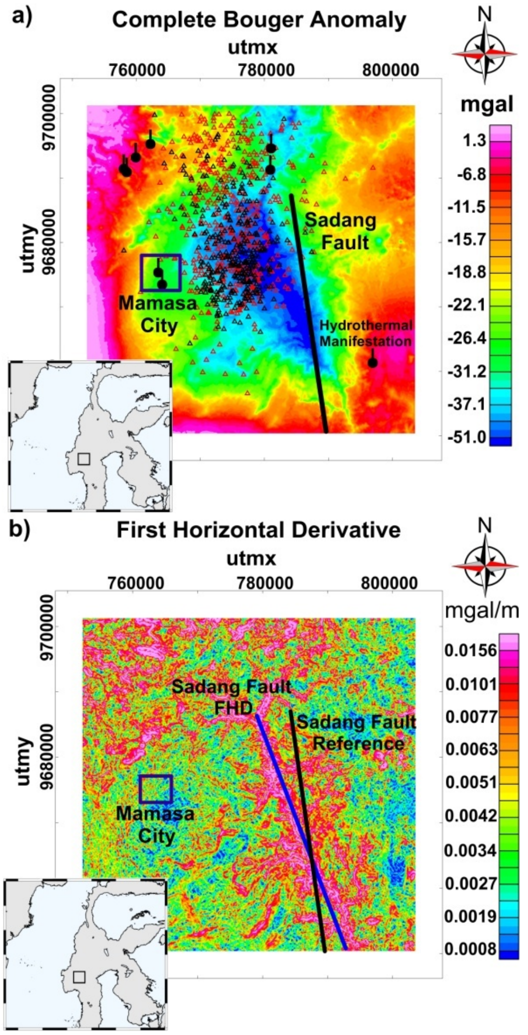

Fig. 3a) Complete Bouguer anomaly (CBA) map; relocated earthquakes are symbolized by transparent black triangles. b) First horizontal derivative (FHD) map with the blue line predicted fault compared to the black line Sadang Fault reference.

The manifestation of hot springs is strongly related to the presence of geological structures [25-27]. Furthermore, the manifestation of hot springs around the earthquake swarm shows the hydrothermal effect. It is believed to strongly influence the occurrence of the earthquake swarm. The volcanic activity has also triggered an earthquake swarm by activating the Sumatra [28,29], Jailolo, and North Maluku Faults [1,30]. According to Suhanto and Bakrun [22] and Idral [31], Mamasa is one of the geothermal prospect areas in Sulawesi. Its hot springs form a semicircular lineament and have a temperature within 42-57 °C. Moreover, the estimated subsurface temperature is only approximately 120 °C [22].

4.2 Palu Earthquake

The modeling of the Palu earthquake static pressure on 28 September 2018 was conducted for only the mainshock [32]. This study combines 11 earthquakes around Palu since their locations and times of occurrence are close together. Furthermore, their foreshock, mainshock, and aftershock are all analyzed (see Table 2). The symbols in Table 2 are depth (*D*), magnitude (*M*), strike (ϕ), dip (δ), rake (λ), fracture length (L), and fracture width (*W*). Fracture length and width values are obtained from the formulation of the magnitude and type of fault relationship with geometry [18].

The global CMT hypocenter is a centroid, not the point of the earthquake (see Table 2 and Figure 4a). Therefore, centroids are used to calculate model fault locations by Coulomb stresses. Furthermore, Figure 4b shows that the Mamasa earthquake zone received a Coulomb pressure of 0.024 to 0.057 bar. These pressures are less than the threshold created by Stein [33], which is 0.1 bar. Therefore, the Palu earthquake did not significantly affect the Mamasa swarm.

Table 2. Earthquake parameters for Coulomb stress calculation.

No	Date	Time	Lat	Long	*D*	*M*	ϕ	δ	λ	*L*	*W*
1	28/09/2018	7:00:02	-0.25	119.89	12	6.1	369	66	-14	15.41	7.73
2	28/09/2018	8:24:57	-0.4	120.02	12	5.2	181	77	-1	3.84	3.47
3	28/09/2018	10:02:59	-0.72	119.86	12	7.6	348	57	-15	156.54	29.32
4	28/09/2018	21:24:01	-1.44	120.22	12	5	127	59	4	2.82	2.91
5	29/09/2018	7:40:10	-1.51	120.15	14	5	101	38	-69	2.68	2.85
6	29/09/2018	10:30:17	-1.43	120.19	12	5.1	116	37	-56	3.12	3.18
7	30/09/2018	14:38:43	-1.25	120.24	26	5.1	111	35	-86	3.12	3.18
8	01/10/2018	5:43:34	0	119.65	15	5.3	311	27	12	4.48	3.79
9	01/10/2018	23:46:40	-0.56	119.88	15	5.3	349	38	-3	4.48	3.79
10	02/10/2018	4:59:26	-1.44	119.95	15	5.4	115	13	6	5.23	4.15
11	22/10/2018	16:07:48	-1.65	120.23	22	5.1	312	76	-18	3.29	3.18

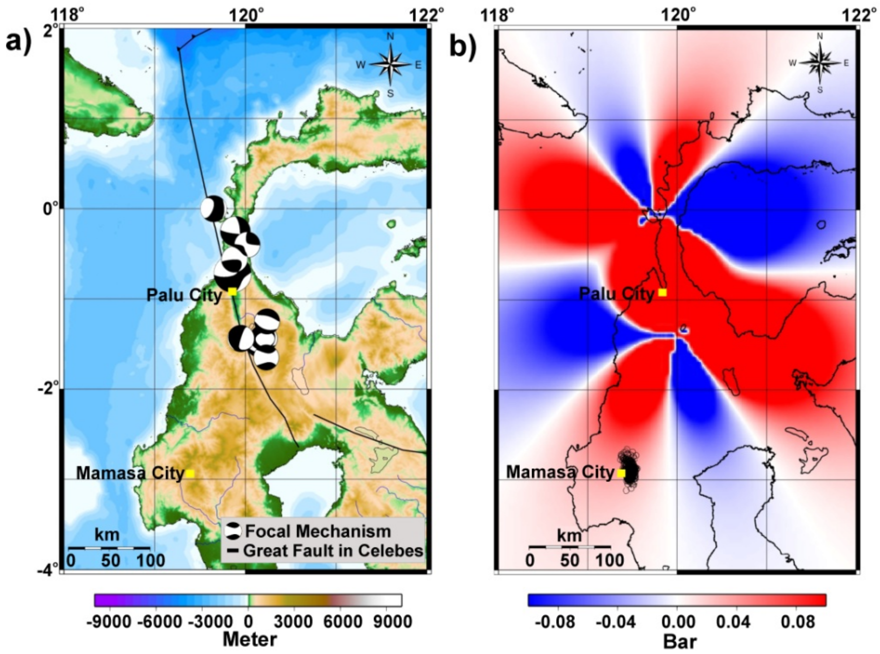

Fig. 4a) Map of the focus mechanism of the Palu earthquake series model. b) Coulomb stress map of the Palu earthquake series. The red zone is the compression zone, while the blue zone is the tension zone.

4.3 Preliminary Seismic Hazard Assessment

The geological profile in Figure 5 shows that the Mamasa region is dominated by intrusive rock layers [19]. There are 5 types of layer structures in this area, including Tmpi (intrusive rocks), Kls (Latimojong Formation), Tmtv (Talaya volcanic rocks), Qbt (Barupu tuff), and Qf (alluvial fan deposits). Furthermore, the cross-section shows that there is a very thick layer (thousands of meters) of granite in Mamasa. The dominance of granite and the thin layer of sediment make the city an area with a low damage potential during an earthquake.

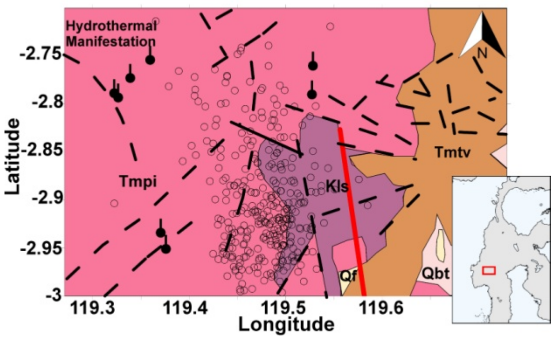

Fig. 5 Geological map of the Mamuju sheet with fractured or fault structures in dashed lines. The red line is the Sadang Fault reference.

The thicker the sediment is, the higher the amplification value and the higher the risk of damage from an earthquake [34]. In addition, the dominance of granite and thin sediment layers makes the depth of the basement very shallow. The shallower the depths are, the higher the dominant frequency of seismic waves [35]. A high dominant frequency lowers the risk in the earthquake area.

5. CONCLUSION

The Mamasa earthquake swarm that occurred from November 2018 to February 2019 was not affected by the Palu earthquake on September 28. This swarm was generated due to two causes, namely, the existence of a local fault in northeastern Mamasa city and hydrothermal activity around the area. Furthermore, the position of this local fault is parallel to the west, and the local fault is not shaped like the Sadang Fault. The presence and position of the Sadang Fault has been verified by FHD gravity data. It appears to extend to the southeast and out of the study area, and it seems to be different from the local fault. For preliminary seismic hazard assessment, Mamasa city is known to have a low risk of damage when shaken by an earthquake based on geological data.

6. ACKNOWLEDGMENTS

We would like to thank the BMKG for providing the data and for permission to use the data for this study. Many thanks also to DRPM Universitas Indonesia for valuable financial support through the PITTA research grant number of NKB-0441/UN2.R3.1/HKP.05.00/2019.

7. REFERENCES

[1] Passarelli, L., Heryandoko, N., Cesca, S., Rivalta, E., Rasmid, Rohadi, S., Dahm, T., and Milkereit, C., Magmatic or Not Magmatic? The 2015-2016 Seismic Swarm at the Long-Dormant Jailolo Volcano, West Halmahera, Indonesia. Frontiers in Earth Science Vol.6, 2018, pp. 79.

[2] Gunawan, M.T., Kusnandar, R., Supendi, P., Nugraha, A. D., Puspito, N. T., Daryono, D., Sahara, D. P., and Zulfakriza, Z., Analysis of swarm earthquakes around Mt. Agung Bali, Indonesia prior to November 2017 eruption using regional BMKG network. Geoscience LettersVol.7,2020, pp. 14.

[3] Heinicke, J., Fischer, T., Gaupp, R., Götze, J., Koch, U., Konietzky, H., and Stanek, K. P., Hydrothermal alteration as a trigger mechanism for earthquake swarms: the Vogtland/NW Bohemia region as a case study. Geophysical Journal International, Vol. 178 Issue 1, 2009, pp. 1-13.

[4] Megies, T., and Wassermann, J., Microseismicity observed at a non-pressure-stimulated geothermal power plant. Geothermics, Vol. 52, 2014, pp. 36-49.

[5] Vavryčuk, V., and Hrubcová, P., Seismological evidence of fault weakening due to erosion by fluids from observations of intraplate earthquake swarms, J. Geophys. Res. Solid Earth, Vol. 122, Issue 5, 2017, pp. 3701– 3718.

[6] Supendi, P., Nugraha, A.D., Widiyantoro, S., Abdullah, C.I., Puspito, N.T., Palgunadi, K.H., Daryono, D., and Wiyono, S.H., Hypocenter relocation of the aftershocks of the Mw 7.5 Palu earthquake (September 28, 2018) and swarm earthquakes of Mamasa, Sulawesi, Indonesia, using the BMKG network data. Geoscience Letters, Vol. 6, Issue 1, 2019, pp. 1-11.

[7] Badan Pusat Statistik (BPS). Population Census Data 2010 in Mamasa, Sulawesi Barat. 2010. https://sp2010.bps.go.id/index.php/site?id=76&wilayah=Sulawesi-Barat [Accessed on 17 November 2019]

[8] Waldhauser, F., and Ellsworth, W.L., A Double-Difference Earthquake Location Algorithm: Method and Application to the Northern Hayward Fault, California. Bulletin of the Seismological Society of America, Vol.90, Issue 6, 2000, pp. 1353-1368.

[9] Kissling, E., Ellsworth, W.L., Eberhart-Phillips, D., and Kradolfer, U., Initial reference models in local earthquake tomography. Journal of Geophysical Research: Solid Earth, Vol. 99, Issue B10, 1994, pp. 19635-19646.

[10] Rosid, M.S. and Saraswati, C.B., Implementation 3D Inversion of Gravity Data to Identify Potential Hydrocarbon Reservoir Zones in West Timor Basin, Journal of Sains Malaysiana, Vol. 49, Issue 9, 2020, pp. 2065-2072.

[11] Laske, G., Masters., G., Ma, Z. and Pasyanos, M., Update on CRUST1.0 - A 1-degree Global Model of Earth's Crust, Geophys. Res. Abstracts, 15, Abstract EGU2013-2658, 2013.

[12] Kennett B.L.N. and Engdahl E.R., Travel times for global earthquake location and phase association. Geophysical Journal International, Vol. 105, Issue 2, 1991. pp. 429-465.

[13] Hirt, C., Claessens, S., Fecher, T., Kuhn, M., Pail, R., and Rexer, M. (2013). New ultrahigh-resolution picture of Earth's gravity field. Geophysical Research Letters, Vol. 40, Issue 16, 2013, pp. 4279-4283.

[14] Jarvis, A., Guevara, E., Reuter, H.I., and Nelson, A., Hole-filled SRTM for the globe Version 4. 2008 http://srtm.csi.cgiar.org [Accessed on 15 March 2019].

[15] Parasnis, D.S., (1952). A study of rock densities in the English Midlands. Geophysical Supplements to the Monthly Notices of the Royal Astronomical Society, Vol. 6, Issue 5, 1952, pp. 252-271.

[16] Dziewonski, A.M., Chou, T.A., and Woodhouse, J.H., Determination of earthquake source parameters from waveform data for studies of global and regional seismicity. Journal of Geophysical Research: Solid Earth, Vol. 86, Issue B4, 1981, pp. 2825-2852.

[17] King, G.C.P., Stein, R.S., and Lin, J., (1994). Static stress changes and the triggering of earthquakes. Bulletin of the Seismological Society of America, Vol. 84, Issue 3, 1994, pp. 935-953.

[18] Wells, D.L., and Coppersmith, K.J., New empirical relationships among magnitude, rupture length, rupture width, rupture area, and surface displacement. Bulletin of the Seismological Society of America, Vol. 84, Issue 4, 1994, pp. 974-1002.

[19] Ratman, N., and Atmawinata, S., Geological Map of Mamuju Sheet, Sulawesi. Geological Research and Development Center, Bandung, Indonesia, 1993.

[20] Kuiper E., River Morphology. In: Water Resources Development. Springer, Boston, MA., 1965.

[21] Hamilton, W.B., Tectonics of the Indonesian Region vol. 1078. US Govt. Print. Off., Washington, 1979.

[22] Suhanto, E., and Bakrun, Studi kasus lapangan panasbumi non vulkanik di Sulawesi: Palu, Mamasa, Parara, dan Mangolo. Technical report in Bahasa Indonesia (Abstract provided in English), Kolokium Hasil Kegiatan

Inventarisasi Sumber Daya Mineral, 2003.
[23] Ziyad, E.R., Relationship between tectonic activity, fluvial system and river morphology in the Dohuk catchment, Iraqi Kurdistan. Geomorphologie, Vol. 20, Issue. 1, 2014, pp. 91-100.
[24] Wu, G., Tan, H., Yang, G., and Shen, C., Research on the relationship between geophysical structural features and earthquakes in Mid-Yunnan and the surrounding area. Geodesy and Geodynamics, Vol. 6, Issue 5, 2015, pp. 384-391.
[25] Ibrahim, M.O., Geothermal Manifestations and Structures in Innstidalur and Middalur, SW-Iceland. Geothermal Training Programme. Orkustofnun, Grensásvegur 9, IS-108 Reykjavík, Iceland, Reports 2004, Number 14, 2004, pp. 307-324.
[26] Mandradewi, W. and Herdianita, N.R. Characteristics of Surface Manifestation, Cisolok, Sukabumi, West Java: With Relation to Cisolok Geothermal System. Proceedings World Geothermal Congress. 2010.
[27] Setyawan, A., Yudianto, H., Nishijima, J., and HakimS. (2015). Horizontal Gradient Analysis for Gravity and Magnetic Data Beneath Gedongsongo Geothermal Manifestations, Ungaran, Indonesia. Proceedings World Geothermal Congress. 2015.
[28] Ramdhan, M., and Nugraha, A.D., Study of seismicity around Toba area based on relocation hypocenter result from BMKG catalogue. AIP Conference Proceedings Vol. 1554, Issue 1, 2013, pp 242-244.
[29] Nugraha, A.D., Supendi, P., Widiyantoro, S., Daryono, D., and Wiyono, S., Earthquake swarm analysis around Bekancan area, North Sumatra, Indonesia using the BMKG network data: Time periods of February 29, 2015 to July 10, 2017. AIP Conference Proceedings Vol. 1987,2018, pp. 020092.
[30] Nugraha, A.D., Shiddiqi, H.A., Widiyantoro, S., Puspito, N.T., Triyoso, W., Wiyono, S., Daryono, Wandono, and Rosalia, S. Hypocenter Relocation of Earthquake Swarm in West Halmahera, North Molucca Region, Indonesia by using Double-Difference Method and 3D Seismic Velocity Structure. IOP Conf. Series: Earth and Environmental Science Vol. 62, 2017, pp. 012053.
[31] Idral, A., Potency of Non Volcanic Hosted Geothermal Resources in Sulawesi-Indonesia. Proceedings of World Geothermal Congress. 2010.
[32] Hui, G., Li, S., Wang, P., Suo, Y., Wang, Q., and Somerville, I.D., Linkage between reactivation of the sinistral strike-slip faults and 28 September 2018 Mw7.5 Palu earthquake, Indonesia. Science Bulletin, Vol. 63, Issue 24, 2018, pp. 1635-1640.
[33] Stein, R.S., The role of stress transfer in earthquake occurrence. Nature Vol. 402, Issue 6762, 1999, pp. 605-609.
[34] Ningrum, R.W. Fauzi, H., Suryanto, W., and Mei, E.T.W., Seismic Hazard Measurement of Earthquake Swarms Activity Based on Horizontal Vertical to Spectral Ratio Analysis (HVSR) in West Halmahera, Indonesia. IOP Conf. Series: Earth and Environmental Science Vol. 279, 2019, pp. 012041.
[35] Parolai. S., Bormann, P., and Milkereit, C., Assessment of the natural frequency of the sedimentary cover in the Cologne area (Germany) using noise measurements. Journal of Earthquake Engineering, Vol. 5, Issue 4, 2001, pp. 541– 556.